

# Selective ratiometric detection of H<sub>2</sub>O<sub>2</sub> in water and in living cells with boronobenzo[*b*]quinolizinium derivatives†

 Roberta Bortolozzi,<sup>a</sup> Sebastian von Gradowski,<sup>b</sup> Heiko Ihmels,\*<sup>b</sup> Katy Schäfer<sup>b</sup> and Giampietro Viola<sup>‡,a</sup>

 Cite this: *Chem. Commun.*, 2014, 50, 8242

 Received 27th March 2014,  
Accepted 6th June 2014

DOI: 10.1039/c4cc02283a

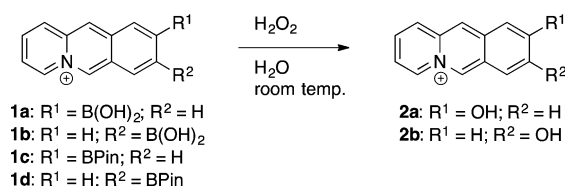
[www.rsc.org/chemcomm](http://www.rsc.org/chemcomm)

**Boronbenzo[*b*]quinolizinium derivatives exhibit several favorable properties for the fluorimetric detection of hydrogen peroxide, namely quantitative transformation to a product whose emission maximum is well separated from the one of the substrate, water solubility, and the ability to operate in living cells.**

Reactive oxygen species (ROS), such as *e.g.* hydrogen peroxide, singlet oxygen, the hydroxyl radical, the superoxide anion, peroxyxynitrite, or ozone,<sup>1</sup> have fundamental functions in health and disease related processes.<sup>2</sup> Specifically, increased concentrations of H<sub>2</sub>O<sub>2</sub> may cause oxidative damage of cellular proteins, ageing and diseases such as cancer or diabetes.<sup>3</sup> Therefore, the detection of H<sub>2</sub>O<sub>2</sub> and other ROS is a challenging and important task in biological and chemical research. Along these lines, fluorescent probes have been established as sensitive and selective tools for the detection of H<sub>2</sub>O<sub>2</sub>.<sup>4a</sup> Fluorescent light-up probes offer one approach to respond to H<sub>2</sub>O<sub>2</sub> by an emission increase.<sup>5</sup> These intensity-based probes may have practical advantages; however, they suffer from the fact that the emission intensity is also effectively influenced by other internal and external factors.<sup>4b</sup> A complementary approach towards fluorimetric detection of ROS is based on ratiometric probes operating at two different detection wavelengths that enable an accurate internal calibration.<sup>6</sup> In this context aryl boronates were identified as probe molecules whose selective reaction with H<sub>2</sub>O<sub>2</sub> may be employed for the development of ratiometric fluorescent probes.<sup>7</sup> In general the transformation of the boronic acid (ester) group into an hydroxy functionality results in a significant change of the absorption and emission properties of the fluorophore thus

enabling a ratiometric analysis. Based on this principle, several ratiometric H<sub>2</sub>O<sub>2</sub>-sensitive probes were developed.<sup>8</sup> Nevertheless, the development of novel ratiometric fluorescent chemosensors for the detection of H<sub>2</sub>O<sub>2</sub> is still an important goal, especially those with sufficient water solubility. The latter is an essential requirement for studies in biological media. In this context we have established the benzo[*b*]quinolizinium as a versatile, water-soluble fluorophore for fluorimetric detections.<sup>9</sup> In addition, we have discovered that the hydroxy-substituted benzo[*b*]quinolizinium derivative **2b** has fluorosolvatochromic properties with a large red-shift of the emission band in water (600 nm).<sup>10</sup> At the same time, the 9-boronobenzo[*b*]quinolizinium (**1a**) exhibits the same emission bands as the parent compound (417 nm).<sup>11</sup> Considering this large difference of emission color of borono- and hydroxy-substituted derivatives we proposed that the formation of the latter by the reaction of H<sub>2</sub>O<sub>2</sub> with boronobenzo[*b*]quinolizinium derivatives may be monitored by a drastic shift of the emission wavelength. Meanwhile, it was shown that resembling quinolinium-type boronic acid esters may indeed be used for that purpose.<sup>8a</sup> Herein, we will demonstrate that the boronic acids and ester derivatives **1a–d** may be generally employed as ratiometric fluorescence probes for the detection of H<sub>2</sub>O<sub>2</sub> in aqueous solution and in living cells (Scheme 1).

The benzo[*b*]quinolizinium derivatives **1a,b** and **2a,b** were synthesized by the cyclodehydration method,<sup>12</sup> and the two acid derivatives **1a,b** were transformed to the corresponding pinacolboronates **1c,d** (*cf.* ESI†). Known compounds (**1a**, **2a,b**) were identified by comparison with literature data.<sup>10,11,12b</sup> All new compounds (**1b–d**) were characterized by <sup>1</sup>H-NMR and <sup>13</sup>C-NMR spectroscopy, mass spectrometry and elemental analysis (*cf.* ESI†).



**Scheme 1** Reaction of boronobenzo[*b*]quinolizinium derivatives **1a–d** with H<sub>2</sub>O<sub>2</sub>.

<sup>a</sup> Dipartimento di Salute della Donna e del Bambino, Laboratorio di Oncoematologia, University of Padova, via Giustiniani 2, I-35128 Padova, Italy

<sup>b</sup> Department Chemie - Biologie, Universität Siegen, Adolf-Reichwein-Str. 2, 57068 Siegen, Germany. E-mail: ihmels@chemie.uni-siegen.de

† Electronic supplementary information (ESI) available: Experimental procedures, full characterization and NMR spectra, spectroscopic studies. See DOI: 10.1039/c4cc02283a

‡ Author names in alphabetical order that does not reflect the specific contribution of each author.



The absorption spectra of the derivatives **1a–d** in phosphate buffer solution reveal the characteristic long-wavelength absorption band of the benzo[*b*]quinolizinium chromophore<sup>13</sup> with a maximum at 380 nm (**1a,c**) and 377 nm (**1b,d**) (cf. ESI†). The hydroxy-substituted derivatives have absorption maxima at 387 nm (**2a**) and 379 nm (**2b**),<sup>10</sup> along with a weak, very broad redshifted charge transfer (CT) band at *ca.* 450 nm.<sup>10</sup> The emission properties of the boronic acid derivatives **1a–d** resemble the ones of the parent benzo[*b*]quinolizinium ( $\lambda_{\text{fl}} = 410\text{--}415$  nm;  $\Phi_{\text{fl}} = 0.03\text{--}0.12$ ). In contrast, the fluorescence maxima of the hydroxybenzo[*b*]quinolizinium derivatives are significantly redshifted with maxima at 527 nm (**2a**) and 600 nm (**2b**).<sup>10</sup>

The reaction of the derivatives **1a–d** with  $\text{H}_2\text{O}_2$  in buffer solution produced the corresponding hydroxybenzo[*b*]quinolizinium derivatives **2a** and **2b** (Scheme 1). Most notably, in the case of **1a–d** the  $^1\text{H-NMR}$ -spectroscopic analysis of the reaction revealed a quantitative transformation with no detectable side products (cf. ESI†). The reaction of compounds **1a–d** with  $\text{H}_2\text{O}_2$  in buffer solution was also monitored by emission spectroscopy (Fig. 1). The progress of the reaction is clearly indicated by a continuous decrease of the intensity of the emission maximum of compounds **1a–d** (415 or 417 nm) that is accompanied by the simultaneous increase of a new redshifted emission band at 527 nm and 600 nm, respectively. The latter emission bands are identical to the ones obtained with authentic samples of the hydroxy-substituted derivatives **2a,b**. The ratios of the intensities of the emission maxima increase by a factor of 17 (**1a**) and 0.7 (**1b**) at 140 min after addition of  $\text{H}_2\text{O}_2$ , as quantified by the term  $I_{\text{red}}/I_{\text{blue}}$ . Control experiments showed that the formation of **2a** and **2b** does not take place in buffer solution in the absence of  $\text{H}_2\text{O}_2$ . The results indicate full conversion of the substrates **1a,b** to the products **2a,b** within 140 min (**1a**) and 160 min (**1b**). The limit of detection was determined to be 3.0  $\mu\text{M}$  for **1a** and 5.9  $\mu\text{M}$  for **1c** (cf. ESI†), which is comparable to that of established probes.<sup>5b,8a,c</sup> The reaction rate was analyzed considering pseudo first-order kinetics according to an established protocol.<sup>8c</sup> By this method, rate constants of  $k_{\text{obs}} = 4.3 \times 10^{-4} \text{ s}^{-1}$  (**1a**) and  $k_{\text{obs}} = 2.9 \times 10^{-4} \text{ s}^{-1}$  (**1b**) were obtained (cf. ESI†). To assess the selectivity of the oxidation reaction of compounds **1a–d** they were also treated with other oxidants, namely  $\text{O}_2^{\bullet-}$ ,  $^1\text{O}_2$ ,  $\text{ClO}^-$ ,  $\text{NO}^\bullet$ , peroxides  $\text{ROO}^\bullet$ ,  $\text{HO}^\bullet$ , and  $\text{ONO}_2^-$ . The reaction was monitored by fluorescence spectroscopy, and the ratiometric analysis,  $I_{\text{red}}/I_{\text{blue}}$ , was used to determine the progress of the reaction (Fig. 2). Notably, the compounds **1a** and **1c** are efficiently oxidized by  $\text{H}_2\text{O}_2$ , whereas the other oxidants only induce the formation of the oxidation product **2a** to marginal or moderate ( $\text{O}_2^{\bullet-}$ ,  $\text{HO}^\bullet$ ,  $\text{ONO}_2^-$ ) extent under resembling reaction conditions. A similar trend was observed for the derivatives **1b** and **1d**, however, the selectivity is less pronounced, and the ratio of  $I_{\text{red}}/I_{\text{blue}}$  is smaller because of the lower emission intensity of the reaction product **2b**.

The ability of the derivatives **1c** and **1d** to detect varying levels of  $\text{H}_2\text{O}_2$  in living cells was assessed. For this purpose, we used HeLa cell lines, *i.e.* an adenocarcinoma that grows as monolayer, and Jurkat cells, *i.e.* leukemia cell lines that grow in suspension. In preliminary experiments the cellular uptake by compound **1c** was evaluated by flow cytometry taking advantage of the intrinsic fluorescence of the compound (cf. ESI†).

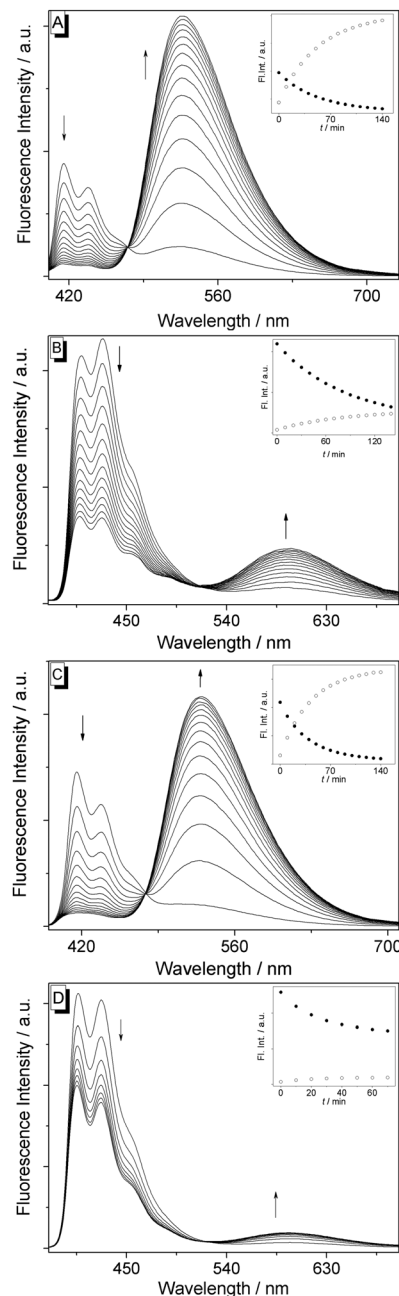


Fig. 1 Fluorimetric monitoring of the reaction of  $\text{H}_2\text{O}_2$  (1.0 mM) with **1a** (A, 10  $\mu\text{M}$ ,  $\lambda_{\text{ex}} = 366$  nm), **1b** (B, 10  $\mu\text{M}$ ,  $\lambda_{\text{ex}} = 361$  nm), **1c** (C, 10  $\mu\text{M}$ ,  $\lambda_{\text{ex}} = 366$  nm), or **1d** (D, 10  $\mu\text{M}$ ,  $\lambda_{\text{ex}} = 366$  nm) in phosphate buffer (0.1 M, pH = 7.4). Arrows indicate the development of emission bands with time. Inset: plot of the fluorescence maxima of **1a–d** (●) and **2a,b** (○) versus time.

The cellular uptake was rapid and reached a plateau after 15–20 min of incubation in Jurkat cells and after 1 h in HeLa cells suggesting an efficient delivery of the compound inside the cells. After 1 h of incubation **1c** and **1d** emit at 450 nm (FL9 channel), while no emission was detectable at 540 nm (FL10 channel) (cf. ESI†). To evaluate the ability of derivatives **1c** and **1d** to respond to  $\text{H}_2\text{O}_2$  in a living cell, HeLa cells were treated with  $\text{H}_2\text{O}_2$  (100  $\mu\text{M}$ ) after the incubation with **1c** and **1d**, and the relative fluorescence intensities of the cells were



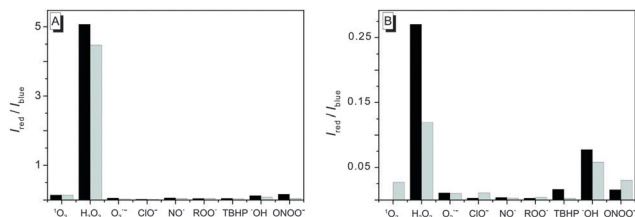


Fig. 2 Ratiometric fluorimetric analysis of the reaction of **1a** (A, black), **1c** (A, grey), **1b** (B, black), and **1d** (B, grey) ( $c = 10 \mu\text{M}$ ) with selected ROS ( $c = 1.6 \times 10^{-4} \text{ M}$ , resp.) in phosphate buffer ( $c = 0.1 \text{ M}$ ,  $\text{pH} = 7.4$ );  $t = 60 \text{ min}$ ; **1a**, **1c**:  $\lambda_{\text{ex}} = 366 \text{ nm}$ , **1b**, **1d**:  $\lambda_{\text{ex}} = 361 \text{ nm}$ ;  $\text{ROO}^{\cdot} = \text{C}_4\text{H}_9\text{N}_2\text{OO}^{\cdot}$ .

analyzed by flow cytometry (Fig. 3). After 10 min the fluorescence intensity of **1c** at 450 nm decreased, and a signal at 540 nm developed (Fig. 3A and B). This development of emission signals may be followed also by a ratiometric analysis (cf. ESI†). In the case of **1d**, however, only the signal at 450 nm disappeared, but no redshifted emission was observed.

Furthermore, we evaluated if **1c** could be useful to detect physiological generation of  $\text{H}_2\text{O}_2$  under pharmacological induction. Thus, both HeLa and Jurkat cells were treated with staurosporine, that is known to induce apoptosis through mitochondrial membrane depolarization. The latter has been associated with mitochondrial production of reactive oxygen species (ROS), in particular  $\text{H}_2\text{O}_2$ .<sup>14</sup> HeLa and Jurkat cells were treated with the drug for 12 h and afterwards incubated with **1c** for 30 min. Subsequent analysis by flow cytometry showed a significant increase of the population of cells that emit at 540 nm in both cell lines (Fig. 4), thus demonstrating the capability of compound **1c** to indicate pharmacologically stimulated formation of intracellular  $\text{H}_2\text{O}_2$ .

In summary we have demonstrated that boronobenzo[*b*]-quinolizinium derivatives exhibit several favorable properties for fluorimetric detection of hydrogen peroxide, namely water solubility,

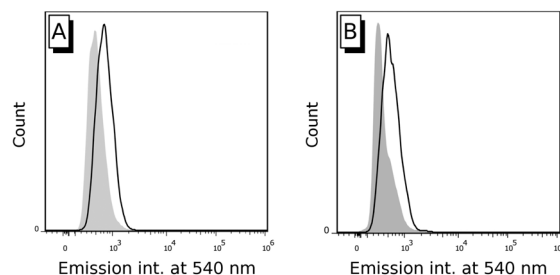


Fig. 4 Flow cytometric analysis of HeLa (A) and Jurkat cells (B) treated for 24 h with staurosporine ( $1 \mu\text{M}$ ) and subsequently incubated with **1c** for 20 min.

quantitative transformation to a product whose emission maximum is well separated from the one of the substrate thus allowing ratiometric analysis, and the general ability to operate in living cells. With respect to a relationship between function and structure, it appears that benzo[*b*]quinolizinium fluorophores, in which the ROS-sensitive borono-functionality as well as the eventually formed hydroxy functionality are linearly conjugated with the pyridinium unit, provide the more effective structural platform for fluorimetric detection as compared to the cross-conjugated system. Specifically, the 9-substituted derivatives **1a** and **1c** exhibit a more pronounced light-up effect and a higher selectivity towards  $\text{H}_2\text{O}_2$  than the 8-substituted ones. It should be noted that these probes may be easily varied by the attachment of other functionalities  $\text{R}^1$  that are transformed to the strongly solvatochromic hydroxy-substituted derivative **2a**.

Generous support by the *Deutsche Forschungsgemeinschaft* is gratefully acknowledged.

## Notes and references

- 1 M. P. Fink, *Curr. Opin. Crit. Care*, 2002, **8**, 6–11.
- 2 (a) P. Niethammer, C. Grabher, A. T. Look and T. J. Mitchison, *Nature*, 2009, **459**, 996–999; (b) G. Groeger, C. Quiney and T. G. Cotter, *Antioxid. Redox Signaling*, 2009, **11**, 2655–2671; (c) E. A. Veal, A. M. Day and B. A. Morgan, *Mol. Cell*, 2007, **26**, 1–14; (d) J. Li, M. Stouffs, L. Serrander, B. Banfi, E. Bettiol, Y. Charnay, K. Steger, K. H. Krause and M. E. Jacobi, *Mol. Biol. Cell*, 2006, **17**, 3978–3988; (e) M. Ushio-Fukai, *Cardiovasc. Res.*, 2006, **71**, 226–235; (f) E. R. Stadtman, *Free Radical Res.*, 2006, **40**, 1250–1258.
- 3 D. Hernández-García, C. D. Wood, S. Castro-Obregón and L. Covarrubias, *Free Radical Biol. Med.*, 2010, **49**, 130–143.
- 4 (a) C. C. Winterbourn, *Biochim. Biophys. Acta*, 2014, **1840**, 730–738; (b) Y. H. A. Liu and X. B. Liao, *Curr. Org. Chem.*, 2013, **17**, 654–669.
- 5 See e.g. (a) M. Kaur, D. S. Yang, K. Choi, M. J. Cho and D. H. Choi, *Dyes Pigm.*, 2014, **100**, 118–126; (b) K. B. Daniel, A. Agrawal, M. Manchester and S. M. Cohen, *ChemBioChem*, 2013, **14**, 593–598; (c) L. Yuan, W. Lin, Y. Xie, B. Chen and S. Zhu, *J. Am. Chem. Soc.*, 2012, **134**, 1305–1315; (d) Y. Ahn, K. E. Fairfull-Smith, B. J. Morrow, V. Lussini, B. Kim, M. V. Bondar, S. E. Bottle and K. D. Belfield, *J. Am. Chem. Soc.*, 2012, **134**, 4721–4730; (e) L. Yuan, W. Lin, S. Zhao, W. Gao, B. Chen, L. He and S. Zhu, *J. Am. Chem. Soc.*, 2012, **134**, 13510–13523; (f) N. Kartun-Lifshin, E. Segal, L. Omer, M. Portnoy, R. Satchi-Fainaro and D. Shabat, *J. Am. Chem. Soc.*, 2011, **133**, 10960–10965.
- 6 (a) C.-Y. Chen and C.-T. Chen, *Chem. – Eur. J.*, 2013, **19**, 16050–16057; (b) A. R. Lippert, G. C. V. De Bittner and C. J. Chang, *Acc. Chem. Res.*, 2011, **44**, 793–804; (c) A. E. Albers, V. S. Okreglak and C. J. Chang, *J. Am. Chem. Soc.*, 2006, **128**, 9640–9641.
- 7 (a) Y. H. A. Liu and X. B. Liao, *Curr. Org. Chem.*, 2013, **17**, 654–669; (b) Z. Q. Guo, I. Shin and J. Yoon, *Chem. Commun.*, 2012, **48**, 5956–5967; (c) For mechanism, see: H. G. Kuivila and A. G. Armour, *J. Am. Chem. Soc.*, 1957, **79**, 5659.

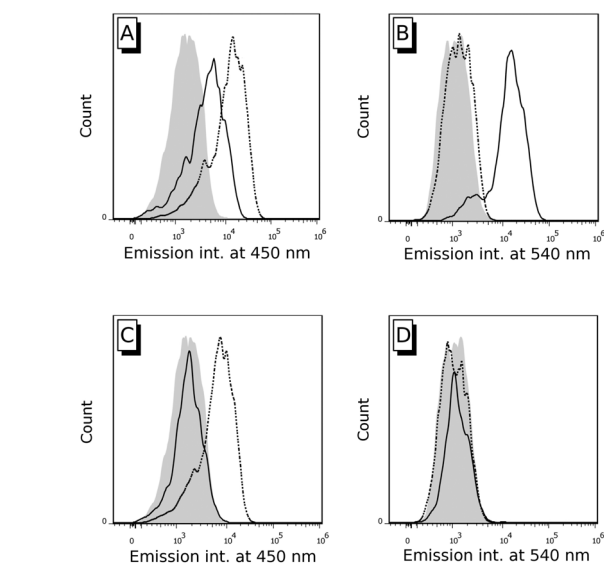


Fig. 3 Flow cytometric analysis of HeLa cells incubated with **1c** (A and B) and **1d** (C and D) for 1 h (dotted lines) treated with  $100 \mu\text{M}$   $\text{H}_2\text{O}_2$  and then re-analyzed after 10 min of incubation (continuous lines). The gray shadows represent untreated cells. The data represent at least 10 000 cells for each analysis.



- 8 (a) S. W. Lee, H.-W. Rhee, Y.-T. Chang and J.-I. Hong, *Chem. – Eur. J.*, 2013, **19**, 14791–14794; (b) G. P. Li, D. J. Zhu, Q. Liu, L. Xue and H. Jiang, *Org. Lett.*, 2013, **15**, 924–927; (c) G. Masanta, C. H. Heo, C. S. Lim, S. K. Bae, B. R. Cho and H. M. Kim, *Chem. Commun.*, 2012, **48**, 3518–3520; (d) D. Srikun, E. W. Miller, D. W. Dornaille and C. J. Chang, *J. Am. Chem. Soc.*, 2008, **130**, 4596–4597; (e) A. E. Albers, V. S. Okreglak and C. J. Chang, *J. Am. Chem. Soc.*, 2006, **128**, 9640–9641.
- 9 (a) R. Bortolozzi, H. Ihmels, L. Thomas, M. Tian and G. Viola, *Chem. – Eur. J.*, 2013, **19**, 8736–8741; (b) M. Tian, H. Ihmels and S. T. Ye, *Org. Biomol. Chem.*, 2012, **10**, 3010–3018; (c) M. Tian, H. Ihmels and K. Benner, *Chem. Commun.*, 2010, **46**, 5719–5721; (d) M. Tian and H. Ihmels, *Chem. Commun.*, 2009, 3175–3177; (e) A. Bergen, A. Granzhan and H. Ihmels, *Photochem. Photobiol. Sci.*, 2008, **7**, 405–407.
- 10 H. Ihmels and K. Schäfer, *Photochem. Photobiol. Sci.*, 2009, **8**, 309–311.
- 11 M. Tian and H. Ihmels, *Synthesis*, 2009, 4226–4234.
- 12 (a) C. K. Bradsher, *Chem. Rev.*, 1946, **46**, 447–499; (b) C. K. Bradsher and J. H. Jones, *J. Am. Chem. Soc.*, 1957, **79**, 6033–6034.
- 13 S. U. D. Saraf, *Heterocycles*, 1981, **16**, 987–1007.
- 14 (a) H. Nohl, L. Gille and K. Staniek, *Biochem. Pharmacol.*, 2005, **69**, 719–723; (b) J. Cai and D. P. Jones, *J. Biol. Chem.*, 1998, **273**, 11401–11404.

